Modeling and simulation of hydrostatic transmission system with energy regeneration using hydraulic accumulator [†]

Triet Hung HO[1] and Kyoung Kwan AHN[2,*]

[1]*Graduate School of Mechanical and Automotive Engineering, University of Ulsan, Ulsan, Korea*
[2]*School of Mechanical and Automotive Engineering, University of Ulsan, Ulsan, Korea*

Abstract

A new hydraulic closed-loop hydrostatic transmission (HST) energy-saving system is proposed in this paper. The system improves the efficiency of the primary power source. Furthermore, the system is energy regenerative, highly efficient even under partial load conditions. It can work in either a flow or pressure coupling configuration, allowing it to avoid the disadvantages of each configuration. A hydraulic accumulator, the key component of the energy regenerative modality, can be decoupled from or coupled to the HST circuit to improve the efficiency of the system in low-speed, high-torque situations. The accumulator is used in a novel way to recover the kinetic energy without reversion of fluid flow. Both variable displacement hydraulic pump /motors are used when the system operates in the flow coupling configuration so as to enable it to meet the difficult requirements of some industrial and mobile applications. Modeling and a simulation were undertaken with regard to testing the primary energy sources in the two configurations and recovering the energy potential of the system. The results indicated that the low efficiency of traditional HSTs under partial load conditions can be improved by utilizing the pressure coupling configuration. The round-trip efficiency of the system in the energy recovery testing varied from 32% to 66% when the losses of the load were taken into account.

Keywords: Hydrostatic transmission; Secondary control; Energy saving; Regenerative systems

---

1. Introduction

A hydraulic system is considered energy-saving system if it has one of the following capabilities. First, it must improve the efficiency of the primary power source of a system, which may be an electric motor or an internal combustion engine in industrial and mobile applications, respectively. Next, it must be a regenerative system that is able to recover energy during deceleration or while a load is lowered. For instance, a system regenerates a vehicle's kinetic energy dissipated by heat transfer via a friction brake during deceleration. The efficiency of the system should also be high over a wide operating range. For example, traditional hydraulic systems using flow valves with fixed displacement are inefficient in cases where the desired velocity and load vary over a wide range, since the excess flow is dissipated via relief valves. According to the above rules, hydrostatic transmission (HST), secondary control systems using constant pressure systems (CPS) combined with flywheels, secondary control systems using impressed

pressure with a hydraulic accumulator CPR, and electro-hydraulic actuators (EHA), have all been considered hydraulic energy-saving systems.

In the HST control problem, the velocity of the hydraulic motor is usually considered as a control variable [1-3]. Many control algorithms have been applied to HST systems; the pertinent studies have shown that the performance of an HST is reasonable for mobile applications whether the system is open or closed. In those studies, only the speed response was considered, but energy utilization and other parameters such as hydraulic pressure in the hose not having been determined. In some mobile applications, such as wheel loaders, an HST with only one variable displacement pump does not satisfy the required torque–speed curve [4, 5]. In such applications, an HST with two variable displacements is required. However, HSTs have a few inherent drawbacks that restrict their use in vehicles or industrial applications. An HST is composed of at least a hydraulic pump and a hydraulic motor, which makes the overall efficiency of the system low compared to that of a mechanical transmission. The efficiency of an HST depends strongly on the load conditions, with significantly low efficiency seen under conditions of partial load, which occur when either the desired velocity or torque is much less than its

maximum value. An HST for low speed and high torque was studied in [6]; the results indicated that the overall leakage losses of the system increase when pressure increases. An open-circuit HST requires an external brake to reduce load speed, and the system is not reversible if there is no directional control valve. To overcome that problem, a closed HST is employed where reversible or braking problems occur. Furthermore, a closed HST has good system performance, but pressure in the return line is often high when reducing the motor speeds. That hydraulic energy is dissipated by heating via over-center valves or an electric power source, which uses the energy to power the cooling system.

If recoverable energy dissipated during the deceleration of a load can be regenerated and reused, then HST systems may be applied more widely. Some energy-recovering hydraulic circuits have been developed for this purpose, such as secondary control systems using common or impressed pressure line CPR [6-12], electro-hydraulic actuators EHA [13], or a constant pressure system (CPS) using a flywheel [14]. Their two main advantages are their energy recovery potentials and their controllable characteristics. However, they also have some disadvantages due to their characteristics. The CPS not only regenerates the kinetic energy of the load, but it also performs the tasks of the engine manager, so it has some energy-saving benefits. Two main drawbacks in a CPS are vibration and noise, which occur when operating the hydraulic pump/motor that drives the flywheel. A closed-loop switching type of CPS also has been proposed as an improvement to the traditional CPS [15-17]. However, to recover and reuse the stored energy, the kinetic energy of the load follows a cycle from the pump, through the motor, to the flywheel and then back from the flywheel to the pump, motor, and load. For a particular load, the motor and pump efficiencies participate twice in the calculation of the round-trip efficiency of a CPS. If the efficiency of one component is low, then the overall round-trip efficiency is very low. The electro-hydraulic actuator (EHA) is another solution. In EHA systems, batteries or capacitors are used to store the kinetic energy of the load [13]. Although an EHA has a high recovery efficiency and good performance, its low specific power and the need for more electric devices sometimes restrict its applications. In heavy duty systems, such as farm tractors or wheel loaders, the addition of electric motors, generators, and batteries in a limited space is not a viable solution.

The CPR system was developed in the early 1980s. Two common lines are employed in the system: a high-pressure line connected with high-pressure accumulators and a low-pressure line connected directly to a tank or low-pressure accumulators. Thus, several secondary units work simultaneously and independently. Pumps are used to control the pressure, while the speed of the load is controlled by adjusting the displacements of the secondary units. By controlling the displacements of the secondary units, the torque at each unit is adjusted, and therefore the speed is controlled. In a CPR system, secondary units can work as motors driving the loads
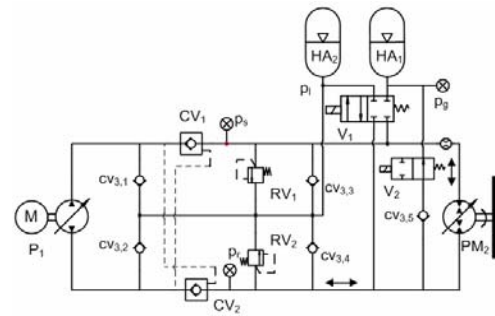

Fig. 1. Schematic of proposed system.

while they also function as pumps regenerating the kinetic energy of the loads. The hydraulic accumulators are used for two functions, storing recovered energy and generating operating pressure. Operating pressure is independent from the external load, which is different from traditional flow coupling. CPR systems have been shown to have good performance as well as energy-saving potentials in some applications [6]. The efficiency of a secondary unit (usually the swash plate machine) varies depending on the load conditions, and is significantly reduced when the load is low. The influence of secondary units on others and the inertia of the fluid (especially for units with large flow rates) are disadvantages of such systems.

This paper proposes an improved closed-loop HST with two hydraulic accumulators (one high pressure and one low pressure). The advantages of a closed-loop HST were realized in the proposed system. The system has the energy recovery potential of a secondary control system and functions both as a CPR system for recovered and reused stored energy and as a traditional HST under full load conditions, which improves not only the efficiency but also the performance of the system. A pump supplies only a load in an HST, which separates a load from other loads. The isolation end effects concept is utilized by determining where the use of different pumps for different loads can improve the efficiency and performance of each load [18].

In the present study, an analytical model of the system based on mathematical equations for each component was developed. The energy utilization and recovery potential of the system was investigated by means of simulations. The paper is organized as follows: Section 2 discusses the properties of the system based on mathematical equations derived by physical modeling. Section 3 analyzes the dynamic response of the system. Section 4 provides the energy utilization analysis, and Section 5 describes the recovery potential of the system. Section 6 presents conclusions.

2. Proposed HST

2.1 System description

Fig. 1 shows a schematic of the proposed system. In comparison to a traditional HST, two directional control valves (V_1, V_2) and two hydraulic accumulators (HA_1, HA_2) are added. The high-pressure accumulator functions as a storage
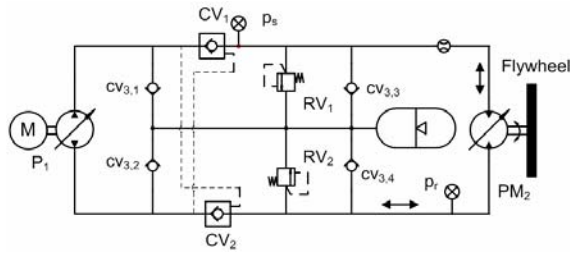
Fig. 2. Flow coupling mode of proposed system.

Fig. 3. Pressure coupling configuration of system.

system or a power supply, while the low-pressure accumulator functions as a low-pressure, high-flow source for the hydraulic pump during recovery time, and boots the system during driving. The functions of the two pilot check valves and the two relief valves are discussed later for each particular configuration. The flywheel functions as an external load.

Hydraulic pump P_1 requires the full range of its displacement, -100% to 100%, while hydraulic pump/motor PM_2 uses only its 0% to 100% of its displacement. Hydraulic pump/motor PM_2 is powered by either hydraulic pump source P_1 or the high-pressure hydraulic accumulator HA_1. By controlling the two directional valves V_1 and V_2, the system is able to operate in distinct configurations.

2.1.1 Flow coupling mode or traditional hydrostatic transmission configuration

When V_1 is OFF and V_2 is ON, the system operates as a closed-loop hydraulic transmission with over-speed protection mechanisms, as in Fig. 2.

The criterion velocity of the flywheel at each instant is determined by the flow coupling principle expressed in Eq. (1).

$$\omega_{fl} = \frac{\omega_p D_p \eta_{vp} \eta_{vm}}{D_m} \qquad (1)$$

where ω_p, D_p, and η_{pv} are the velocity, displacement, and volumetric efficiency of the pump, and D_m and η_{vm} are the displacement and volumetric efficiency of the motor, respectively. However, the actual velocity of the flywheel may differ from the criterion velocity for a real-time system because of the inertia of the load, even if all of the system parameters are determined exactly. Whenever the velocity of the flywheel is greater than the instantaneous criterion velocity, the pressure in return line p_r is high, while that value in the driving/supply line p_s is too low. Pilot check valve CV_2 is then closed, and hydraulic energy in the form of high-pressure fluid is dissipated via the relief valve. That function is similar to that of a hydraulic brake, which reduces the speed of the flywheel under the criterion values. As the speed of the flywheel in an HST is reduced, the kinetic energy of the flywheel is dissipated by braking. In some applications that energy can be substantial, so recovery of it may significantly reduce energy consumption. An inherent characteristic of HSTs is that the overall efficiency of the system is significantly reduced when
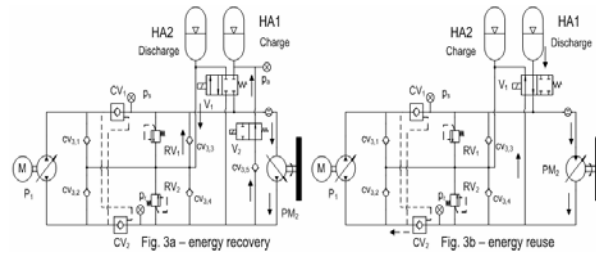
low speed and high torque are required, especially when both requirements are low. The proposed system addresses this issue differently from existing systems, by switching to a pressure coupling configuration to improve the total efficiency of the system.

2.1.2 Pressure coupling-secondary control configuration

When V_1 is OFF and V_2 is ON or when both V_1 and V_2 are ON, the system operates as a pressure coupling system, as shown in Figs. 3(a) and 3(b), respectively. In the configurations, pump P_1 is continuously controlled as a pressure compensated pump or is ON/OFF controlled. The speed of the flywheel is controlled directly by adjusting the displacement of the pump/motor PM_2. In Fig. 3a, the hydraulic pump/motor PM_2 functions as a hydraulic pump that pumps fluid from HA_2 to HA_1. Under this condition, the return line is decoupled from either HA_2 or pump P_1, but is connected directly to HA_1 and acts as a high-pressure line. The driving line is then connected to HA_2 and acts as a one-way low-pressure line. The kinetic energy of the flywheel is transformed to hydraulic energy and is stored in HA_1. When the displacement of the hydraulic machine PM_2 increases, the impeded torque in the shaft of PM_2 also increases, so that the velocity of the flywheel decreases rapidly, and vice versa.

When V_1 is ON, the return line is directly connected to HA_2, while the driving line is connected to HA_1. These then act as the low- and high-pressure lines, respectively. The positions of other valves do not influence the main function of the system. To drive the flywheel, the hydraulic machine PM_2 functions as a hydraulic motor that transforms the potential energy in the HA_1 into the kinetic energy of the flywheel. To accelerate the flywheel, the displacement of PM_2 is increased, and vice versa. In existing energy recovery systems using hydraulic accumulators [6-12], the displacement of PM_2 is reversed over center to change its function from that of a motor to that of a pump. The fluid direction in the system is also reversed, which generates hydraulic shock and noise [14]. In the proposed system, the displacement of PM_2 operates in only one region, and the fluid flows in only one direction. In addition, the use of the accumulator HA_2 and four check valves $CV_{3,1}$, $CV_{3,2}$, $CV_{3,3}$, and $CV_{3,4}$ can avoid the cavitation problem. Therefore, the proposed system overcomes drawbacks experienced when using an HST or CPR alone.

2.2. System modeling

2.2.1 Hydraulic accumulator

The hydraulic accumulator plays an important role in the system. The hydraulic accumulator here is modeled based on its physical attributes. According to [8], the energy balance in the accumulator can be based on the gas present in the accumulator, as in Eq. (2).

$$\frac{dU}{dt} = -p_g \frac{dV}{dt} - m_f c_f \frac{dT}{dt} - hA_w \left(T - T_w \right) \tag{2}$$

where A_w is the effective area of the accumulator for heat convection. For real gas, the time derivative of the internal energy U can be expressed by Eq. (3).

$$\frac{dU}{dt} = m \left[c_v \left(p, T \right) \frac{dT}{dt} + \left(T \left| \frac{\partial p}{\partial T} \right|_v - p_g \right) \frac{dV_g}{dt} \right] \tag{3}$$

where c_v (p,T) is the volume-specific heat as a function of pressure and temperature [J/kg/K], Vg is the specific gas volume [m³/kg], and $\left(\frac{\partial p}{\partial T} \right)_v$ is the partial derivative with a constant gas volume [Pa/K].

For simplicity, the time constants of the accumulator are used and c_v is used instead of c_v (p,T). The temperature of the accumulator is expressed by Eq. (4).

$$\frac{dT}{dt} = \frac{1}{\tau_w} \left(T_{amb} - T_g \left(t \right) \right) - \frac{T(t) q_a(t)}{c_v m} \left| \frac{\partial p_g}{\partial T_g} \right|_v \tag{4}$$

where the accumulator time constant $\tau_w = \frac{mc_v}{\alpha A_c}$ should be measured for each particular type of accumulator, and the partial derivative with respect to time at a constant gas volume is expressed in Eq. (5),

$$\left| \frac{\partial p_g}{\partial T_g}(t) \right|_v = \frac{R}{V_g(t)^2} \left(1 + \frac{2C}{V_g(t) T^3} \right) \left[V_g(t) + B_0 \left(1 - \frac{b}{V_g(t)} \right) \right] \tag{5}$$

The gas pressure is a function of gas temperature and specific volume, as expressed by the Beattie – Bridgman Equation in (6),

$$p_g(t) = \left(\frac{m}{V_g(t)} \right)^2$$
$$\left[RT_g(t) \cdot \left(1 - \frac{mC}{V_g(t) T_g(t)^3} \right) \left(\frac{V_g(t)}{m} + B_0 \left(1 - \frac{mb}{V_g(t)} \right) \right) - A_0 \left(1 - \frac{ma}{V_g(t)} \right) \right] \tag{6}$$

where A_0, B_0, a, b, and R are constants, (given for nitrogen in Table 1).

The gas volume can be estimated from the flow rate into the accumulator using Eq. (7),

$$V_g(t) = V_{0a} + \int_0^t Q_a(t) dt \tag{7}$$

where p_g (t) is the pressure of the gas in the accumulator (which can be considered as the pressure of the fluid in the accumulator), V_g (t) is the gas volume, T_g (t) is the temperature of the gas, m is the mass of the gas, and Q_a is the flow rate into the accumulator.

2.2.2 Hydraulic pumps/motors

Volumetric and mechanical losses of a general axial piston hydraulic machine are used in this study as in [10]. The volumetric losses of a hydraulic machine are expressed by Eqs. (8)-(11).

$$\Delta q_1 = 1.76 \times 10^{-7} \left(\omega / 2\pi \right) + 1.7 \times 10^{-13} \Delta p \tag{8}$$

$$\Delta q_2 = \left(5.10 \times 10^{-14} - 2.83 \times 10^{-14} \alpha \right) \left(\omega / 2\pi \right) \Delta p \tag{9}$$

$$\Delta q_3 = 5.80 \times 10^{-13} \left(\omega / 2\pi \right) D_{max} \Delta p \tag{10}$$

$$Q_{loss} \left(\alpha, \omega, \Delta p \right) = \Delta q_1 + \Delta q_2 + \Delta q_3 \tag{11}$$

The mechanical losses are expressed by Eqs. (12)-(15).

$$\Delta T_1 = 4.27 \times 10^{-2} \left(\omega / 2\pi \right) \tag{12}$$

$$\Delta T_2 = 5.84 \times 10^{-2} \alpha \left(\omega / 2\pi \right) + 8.02 \times 10^{-4} \alpha^2 \left(\omega / 2\pi \right)^2 \tag{13}$$

$$\Delta T_3 = 2.5 \times 10^{-7} \Delta p - 8.1 \times 10^{-15} \Delta p^2 \tag{14}$$

$$T_{loss} \left(\alpha, \omega, \Delta p \right) = \Delta T_1 + \Delta T_2 + \Delta T_3 \tag{15}$$

where α is the displacement ratio, ω is the pump/motor speed, and Δp is the pressure difference between the two ports of each pump/motor. The sources of loss are explained for pump or motor functions as follows.

2.2.2.1 Hydraulic pump

The flow rate from the pump is a nonlinear function of the velocity and displacement of the fluid when volumetric losses are included. The ideal volumetric flow rate of fluid through a pump or a motor is expressed by Eq. (16),

$$Q_{pi} = \alpha \omega D_{max} \tag{16}$$

where α is the displacement ratio that is a proportion of the current displacement to the maximum displacement of the pump or motor. In a practical pump, inlet restriction, leakage,

Table 1. Constant values used in B-B equation.

Constant	Value	Unit
R	296.77	J/ (kgK)
a	$9.33752 \cdot 10^{-4}$	m³/kg
b	$-2.47359 \cdot 10^{-4}$	m³/kg
A_0	$1.74116 \cdot 10^2$	Jm³/kg²
B_0	$1.8007 \cdot 10^{-3}$	m³/kg
C	$5.0948 \cdot 10^{-4}$	m³K³/kg
c_v	754.12	J/ (kgK)

and fluid compressibility all reduce the actual flow rate. Pump volumetric efficiency is defined as the ratio of the actual flow rate to the ideal one expressed by Eq. (17),

$$\eta_{vP} = \frac{Q_i - Q_{loss}}{Q_i} \tag{17}$$

In an ideal pump without any mechanical loss, the mechanical torque required by the pump shaft is expressed in Eq. (18),

$$T_i = \alpha \Delta p D_{max} \tag{18}$$

However, viscous torque, Coulomb torque, and hydrodynamic torque losses always exist for a pump, and therefore must be considered for a practical system. The torque or mechanical efficiency of a hydraulic pump is estimated by Eq. (19),

$$\eta_{tP} = \frac{\alpha D_{max} \Delta p}{\alpha D_{max} \Delta p + T_{loss}} \tag{19}$$

2.2.2.2 Hydraulic motor

The volumetric and mechanical efficiencies are expressed by Eqs. (20) and (21), respectively.

$$\eta_{vM} = \frac{\alpha D_{max} \omega}{\alpha D_{max} \omega + Q_{loss}} \tag{20}$$

$$\eta_{tM} = \frac{\alpha D_{max} \Delta p - T_{loss}}{\alpha D_{max} \Delta p} \tag{21}$$

The actual flow rate into the hydraulic motor is expressed by Eqs. (22),

$$Q_m = \frac{Q_i}{\eta_{vM}} \tag{22}$$

The actual torque generated by the motor is expressed by Eq. (23),

$$T_m = \eta_{tM} \alpha \Delta p D_{max} \tag{23}$$

2.2.2.3 Electro–hydraulic displacement control mechanism of pump/motor

This mechanism is a fifth-order mechanism, although in practical applications a reduced-order model usually is used. We considered it as a first-order system and expressed it as

$$u(t) = \frac{\tau}{K_{sv}} \dot{x} + \frac{1}{K_{sv}} x \tag{24}$$

where u (t) is the electric signal control, τ is the time constant, K_{sv} is the DC gain of the mechanism, and x is the relative swivel angle of the swash plate of the pump/motor.

2.2.3 The connecting lines

In this study, losses due to the length of the pipe were ignored. Continuity equations were used to model the pressure of the fluid in the hose. Depending upon the configuration of the system, two distinct systems can be modeled.

2.2.3.1 Flow coupling configuration

For simplicity, the pressure drop in the check valves is neglected in the driving line, so the pressures before and after check valve CV_1 are similar. Hydraulic accumulator HA_2 is large, so the pressure in the low-pressure line is considered a constant p_l. The dynamic response of the valves can be ignored when compared with that of the flywheel or system pressures. In the driving line, pressure ps is expressed by Eq. (25),

$$\frac{V_0}{\beta} \frac{dp_s}{dt} = Q_{pa} + Q_{b1} + Q_{b2} - Q_{r1} - Q_{ma} \tag{25}$$

where Q_{pa} is the actual flow rate from the pump outlet port, Q_{b1} and Q_{b2} are the boot flow rates, Q_{ma} is the actual flow rate into the inlet port of the motor expressed in Eq. (21), V_0 is the volume of fluid in the hose between the pump and the motor, and Q_{r1} is the flow rate via relief valve RV_1, as expressed by Eq. (26),

$$Q_{r1} = \begin{cases} k_{r1} (p_s - p_{rs1}) \sqrt{p_s - p_l} & if\ p_s > p_{rs1} \\ 0 & else \end{cases} \tag{26}$$

The return line is more sophisticated because the pressures at motor outlet p_r and pump inlet p_{pi} may be different depending on the state of the pilot check valve CV_2. The pressure at the pump inlet port is expressed as in Eq. (27),

$$p_{pi} = \begin{cases} p_r & if\ p_s > p_{cv2} \\ p_l & else \end{cases} \tag{27}$$

where p_{cv2} is the crack pressure of the pilot check valve CV_2. Pressure, p_r, plays an important role in the system dynamics, and is expressed by Eq. (28),

$$\frac{V_0}{\beta} \frac{dp_r}{dt} = Q_{mi} + Q_{b3} + Q_{b4} - Q_{r2} - Q_{pi} \tag{28}$$

where Q_{mi} is the flow rate from the motor outlet port, Q_{b3} and Q_{b4} are the boot flow rates, Q_{pi} is the actual flow rate into the inlet port of the pump expressed in Eq. (16), Q_{r2} is the flow rate via relief valve RV_2, as expressed by Eq. (29),

$$Q_{r2} = \begin{cases} k_{r2} (p_r - p_{rs2}) \sqrt{p_r - p_l} & if\ p_r > p_{rs2} \\ 0 & else \end{cases} \tag{29}$$

where k_{r1} and k_{r2} are the gains of the two relief valves.

2.2.3.2 Pressure coupling configuration

Pressure in the high-pressure line is similar to the gas pressure in HA_1, and pressure in the low-pressure line is similar to the gas pressure in HA_2. Gas pressure or fluid pressure in the

pressure coupling configuration is determined by the accumulator's parameters and the flow rate into it. Flow rate into the high-pressure accumulator is expressed by Eq. (30),

$$Q_a = v_1 \left(Q_{pa} - Q_{r1} - Q_{ma} \right) + v_2 \left(Q_{mi} - Q_{r2} \right) \tag{30}$$

If the dynamic characteristics of the directional control valves are ignored, then v_1 and v_2 are only integer values, as in Eq. (31),

$$v_i = \begin{cases} 0 & \text{if } V_i : OFF \\ 1 & \text{else}, i = 1, 2 \end{cases} \tag{31}$$

Pressure values in the high- and low-pressure lines are expressed by Eqs. (32) and (33), respectively,

$$p_s = \begin{cases} p_g & \text{if } V_1 : ON \\ p_l & V_1 : OFF \end{cases} \tag{32}$$

$$p_r = \begin{cases} p_l & \text{if } V_1 : ON \\ p_g & V_1 : OFF \text{ and } V_2 : ON \end{cases} \tag{33}$$

2.2.4 Flywheel

The dynamic equation of the flywheel is obtained by applying Newton's second law, as in Eq. (34),

$$T_m = J\dot{\omega} + C\omega + T_{ex} \tag{34}$$

where T_m is the torque generated by the hydraulic motor and is presented in Eq. (23), the pressure difference is defined by Eq. (35), J is the moment of inertia of the flywheel, C is the viscous friction coefficient, and T_{ex} is the external torque, which in this study was the braking torque.

$$\Delta p = p_s - p_r \tag{35}$$

3. Simulation

In this study, an HST with flywheel at the FPMI Lab at the University of Ulsan was used in a simulation. Thus, the main parameters of the system were incorporated into the simulation. The maximum displacements of the pump and motor are 55 cc/rev. The speed of the electric motor is 1100 rpm. The setting pressures of the two relief valves are 250 bar. The high-pressure accumulator has a volume of 20 liters and a gas pre-charge pressure of 180 bar. The low-pressure accumulator has a volume of 40 liters and a gas pre-charge pressure of 1 bar. The initial fluid volume in the accumulator is 20 liters, and the initial fluid pressure of the accumulator is 3 bar. The moment of inertia of the flywheel is 4.5 kgm^2.

3.1 Efficiencies of pump and motor

The efficiencies of the pump and motor play an important role in any investigation of the system's energy utilization. Mechanical loss and volumetric loss are the cause of the

(a) Volumetric losses of motor

(b) Mechanical losses of motor

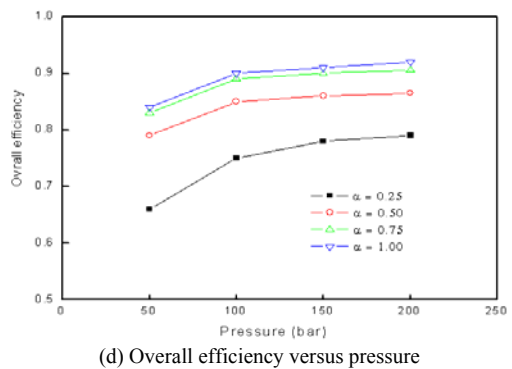

(c) Overall efficiency versus speed
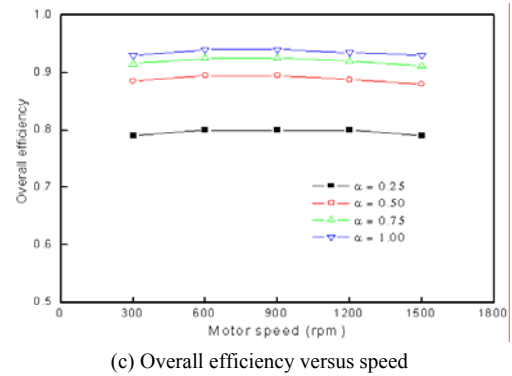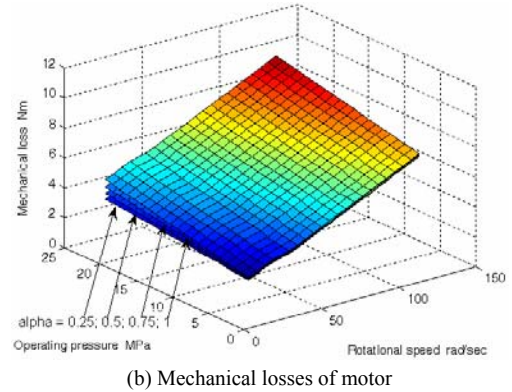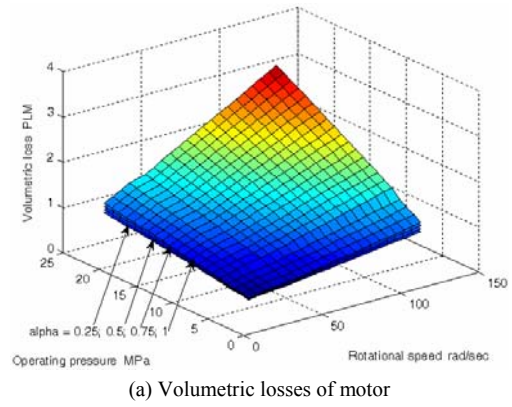

(d) Overall efficiency versus pressure

Fig. 4. Losses and overall efficiency of motor.

pump/motor's inefficiency. The losses of the pump and the motor depend on their operating conditions, the speed, the pressure and the displacement ratio. To survey the losses of

the pump/motor, only the losses of the motor were selected. Figs. 4(a) and 4(b) show the variation of the losses versus the operating conditions of the motor. There are four surfaces, corresponding to displacement ratios 0.25; 0.5; 0.75 and 1. Generally, losses increase when either the operating pressure, speed or displacement ratio of the motor, the operating condition, increases. However, the increase in the losses is small when compared with the increase in the power of the motor under the various operating conditions. Unlike the losses, the efficiency of the motor indicates the relation between the losses and the power of the motor. Thus, the total efficiency of the motor varies over a wide range when the operating conditions vary. For simplicity, two 2-D charts of the overall efficiency are shown in Figs. 4(c) and 4(d) instead of 3-D surfaces. Fig. 4(c) was drawn for a theoretical operating pressure of 200 bar and the displacements of the motor displacement ratios 0.25, 0.5, 0.75, and 1. For a given displacement ratio, the overall efficiency varied insignificantly due to variations in the motor speed. The Fig. shows the variation in the overall efficiency versus the motor speed. The efficiency of the motor increased from 0.8 to 0.94 when α increased from 0.25 to 1.

Fig. 4(d) shows the overall efficiency versus the operating pressure of the motor. The maximum efficiency was about 0.94 at a pressure of 200 bar and $\alpha = 1$. The minimum efficiency was about 0.68 at a pressure of 50 bar and $\alpha = 0.25$. At a given operating pressure, the overall efficiency increased in correspondence to the value of α. For example, at a pressure of 50 bar, the value of the overall efficiency increased from 0.68 to 0.87 as α increased from 0.25 to 1.

### 3.2 Dynamic response of system in open-loop control

To investigate the dynamic characteristics of the system, a step input of the pump displacement was carried out. In this simulation, the directional valves V_1 and V_2 were OFF. The parameters of the system are shown in Fig. 5. Fig. 5(a) shows the speed and pressure of the system corresponding to the step input of the pump displacement. The speed of the system in this case was oscillating in the range of 1000-1100 rpm. The motor accelerated from 0 to 1100 rpm in 2.5 seconds, so the driving line pressure p_s was high (around 250 bar), while the return pressure pr was low. When the speed of the motor decreased, the return pressure pr was high, but the input pressure of the pump remained low. When the speed decreased to 1000 rpm, the driving pressure increased again, so the motor speed also increased. As a result, the pressures in both lines and the speed of the motor were always oscillating, and the system required a closed loop for speed control. Fig. 5(b) shows that the pressure in the accumulator increased gradually from 180 bar to 210 bar as the gas volume in the accumulator decreased from 19.9 liters to 17.8 liters. The temperature of the accumulator increased from 50^0C to 62^0C. The flow rate charged into the accumulator varied from 59.4 LPM to 52.2 LPM when the speed deceased. Fig. 5(c) shows that relief valve RV_1 was opening during the 0-2.5 seconds interval, because the inertial flow rate into the motor was sometimes higher than the deliv-
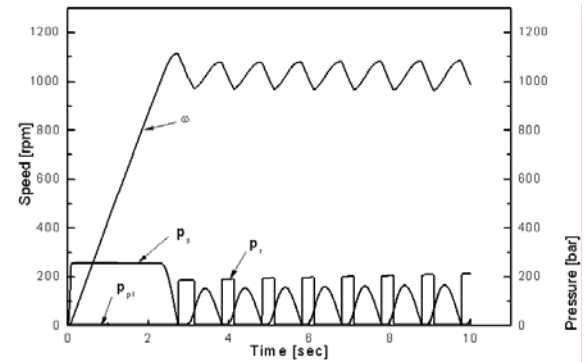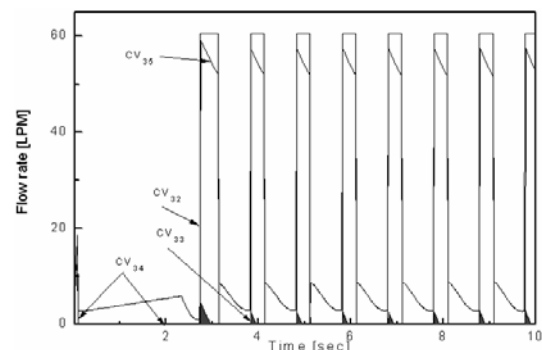

(a) Speed and pressure of system
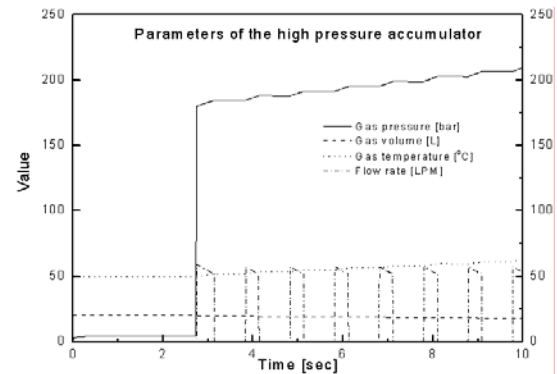
(b) Parameters of high-pressure accumulator
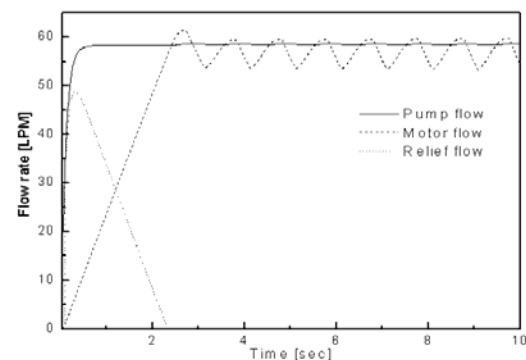
(c) Flow rate of pump, motor and relief valve

(d) Flow rates of check valves

Fig. 5. Characteristic of hydraulic components.

ery of the pump, and the excess flow was delivered via check valve c_{v33}. When the accumulator was charged, the return line

was disconnected between the pump and the motor. The suction port of the pump was connected to the low-pressure accumulator via check valve c_{v32}. Because of the volumetric losses of the pump and the motor, the flow rate via check valve c_{v32} was always greater than the flow rate via check valve c_{v35} or that of the charged fluid into the high-pressure accumulator. All results from Fig. 5 agree with the analytical description in Section 2.1.
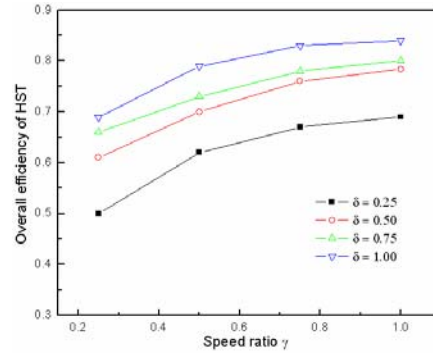
4. Energy utilization of system

4.1 Analysis of energy utilization of system in different configurations

This study focuses on a power drive system only, rather than a total system, such as a hydraulic hybrid vehicle that includes a power drive system and a car chassis. As is known, a representative speed or position trajectory depends on a particular application system, so an analysis of efficiency based on a trajectory restricts the signification of a power drive system analysis. Thus, a survey of a power drive system based on each pair of (γ, δ) is preferable as a scheme for showing the general efficiency characteristics of such a system, for which (γ, δ) are defined as the ratios of the measured speed or torque to their maximum values, respectively. Besides, for a given value of (γ, δ), the efficiency of the system may vary in different configurations. Therefore, this section investigates the relation between the efficiency of the system and (γ, δ) for different configurations. The results of this kind of analysis, therefore, should be considered as the basis of any design for a hybrid-system supervisory controller that achieves the highest overall system efficiency. For instance, the proposed HST system can be employed for a hydraulic hybrid vehicle where a speed trajectory needs to be analyzed. Any speed trajectory of a vehicle can be described in terms of the (γ, δ) of the drive system for each time period if a power analysis approach such as the quasi-static approach is employed [19]. The speed trajectory of the vehicle as analyzed may vary in different regions of the (γ, δ) plane. The use of a fixed control configuration, then, may not guarantee high-efficiency operation of the vehicle over the entire trajectory. In this case, a supervisory controller should be designed to select the configuration according to each (γ, δ).

The maximum power of the system was 18 kW, corresponding to a maximum speed and torque of 1000 rpm and 180 Nm, respectively. Two configurations with three control strategies were examined: flow coupling with closed-loop control, pressure coupling with constant pressure control, and ON/OFF pump control settings changes. For simplicity, these configurations are designated the HST, CPS, and ON/OFF modes, respectively. Due to volumetric losses of the pump and motor, the traditional PID controller was used to ensure the desired speed of the motor in the HST mode. For the CPS mode, the pump was controlled to maintain the pressure in the high-pressure line at about 250 bar, which allows the motor to work at the maximum speed and torque. The motor was con-
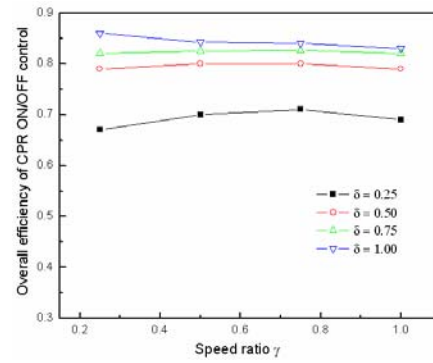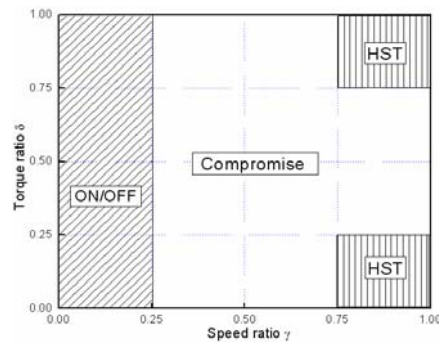

(a) Efficiency of ON/OFF mode

(b) Efficiency of HST mode
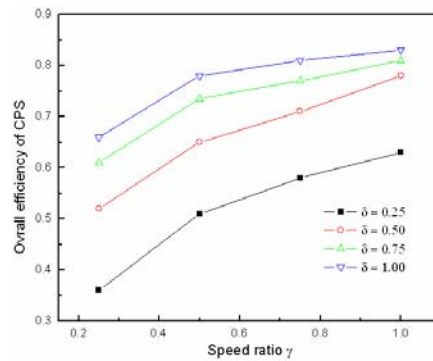
(c) Efficiency of CPS mode

(d) Recommendation of strategy utilization

Fig. 6. Primary energy utilization of system.

trolled to achieve the desired velocity by adjusting its displacement according to the secondary control principle. This principle is described in more detail in [7], and the system

performance is beyond the scope of this article. Thus, both the pump and motor controllers employed were simple PID controllers. Finally, the ON/OFF mode was utilized as follows. The pump controller, an ON/OFF controller feeding back the pressure in the high-pressure line controlled the hydraulic pump to work in maximum displacement until the pressure in accumulator HA1 reached 260 bar, after which it was adjusted to zero. Whenever the flywheel was driven by hydraulic power, the pressure in HA_1 decreased. The pump was controlled to work in maximum displacement when the pressure in HA_1 was down to 240 bar, and the motor controller was also a PID controller.

The results are shown in Figs. 6(a), 6(b), and 6(c); Fig. 6(d) shows the system mode results for the torque and speed ratios, and indicates the recommended mode (HST). The figures show that the ON/OFF control always achieves a higher efficiency than the other control strategies. Under most of the conditions (especially at low torque ratios) the CPS mode had a low overall efficiency of about 0.36 for $\delta = 0.25$ and $\gamma = 0.25$, while those values in the HST and ON/OFF modes were 0.5 and 0.66, respectively. The HST mode dominated for high values of the speed ratio γ; when $\delta = 1$, the overall efficiency varied within the 0.69-0.84 range, depending on the torque ratio δ.

Fig. 6(d) shows that when γ was less than 0.25, the ON/OFF control strategy was better than the others but that the HST dominated when γ was high and δ was low or when both γ and δ were high. For high values of both γ and δ, the ON/OFF and HST modes showed high efficiencies, but the pump was switched with high frequency for the ON/OFF mode, so the HST (with nearly constant values of both pump and motor displacement) was recommended. The other conditions did not significantly differ among the three control strategies.

4.2 Partial loads analysis

Based on the simulation analysis, the scenario of a partial load was investigated for two configurations and three control strategies. The condition entailed low-speed and high-torque requirements with speed and torque values of 250 rpm and 180 Nm, respectively. The parameters of the system in the flow coupling configuration are shown in Fig. 7. The pressure in the CPS mode was controlled at a constant 250 bar, while the pressure in the HST mode was 219.5 bar, according to the 180 Nm of torque at the motor shaft. As shown in the figure, the displacement ratios of the pumps and motors were [0.276, 1] and [0.247, 0857] in the HST and CPS modes, respectively. The pump torques were 61 Nm and 62.8 Nm in the HST and CPS modes, respectively, owing to the different values of the motor and pump torque losses. The torque losses of the motors in both modes were always smaller than those of the pumps. The volumetric losses were small compared with the torque losses for both the pump and the motor. In 80 seconds, the losses of the pump were much greater than those of the motor for both modes, with values of [148.4; 23.3] and [153.4; 23.8] kJ in the HST and CPS modes, respectively. For the
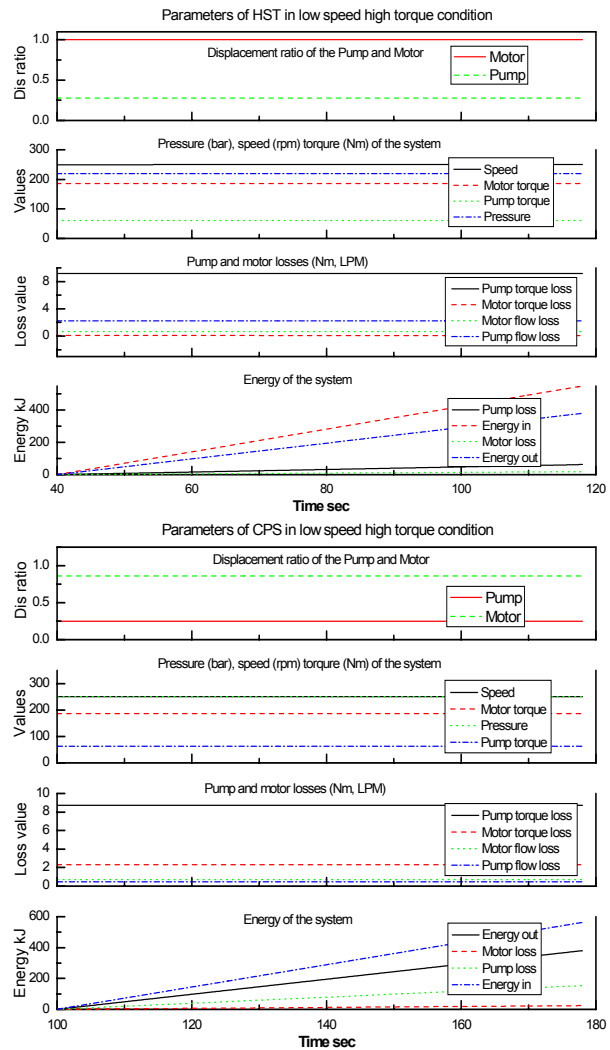

Fig. 7. Parameters of system in HST and CPS modes.

CPS mode, the total energy input and output were 563.52 kJ and 380.41 kJ, respectively, and the overall efficiency was about 0.67. For the HST mode, those values were 551.3 kJ, 380.41 kJ, and 0.69, respectively. There was no significant difference between the two configurations for the low-speed, high-torque condition.

The parameters of the pressure coupling configuration and the ON/OFF control under the partial load conditions are shown in Fig. 8. In this control strategy, the displacements of both the pump and the motor were varied. Fig. 8 shows that displacement of the motor varied by about 0.85, while that of the pump was either 0 or 1. The pump intermittently supplied the motor; whenever the pump was shut OFF, the motor was powered by the accumulator. When the pump was ON, the flow rate delivered from the pump was greater than that required by the motor, so excess flow was sent to the accumulator. Pressure in this mode varied depending on the gas volume of the accumulator, and the speed of the motor oscillated around the desired speed. As shown in the figure, the torque and volumetric losses of the motor were similar to those in the

HST and CPS modes. In this mode, the torque and flow losses of the pump were not much different from those in the HST and CPS modes, but the losses occurred when the pump was ON. The total loss of the pump was reduced to 34 kJ, compared to 148.4 kJ and 153.4 kJ in the HST and CPS modes, respectively. The total loss of the motor in this mode was 19.8 kJ, the total energy input was about 433.8 kJ, and the overall efficiency was about 0.87. Finally, the use of the ON/OFF mode under the low-speed, high-torque condition saved 111 kJ and 123.6 kJ compared with the HST and CPS modes for 80 seconds, respectively.

5. Energy recovery potential of system

5.1 Characteristics of flywheel

The key to energy recovery is the flywheel, so its characteristics were considered before investigating the energy recovery potential of the system. The kinetic energy of the flywheel is lost gradually, without any braking effect, due to friction. The energy loss is dependent on the particular system, and it can be taken into account when analyzing the regenerative cycling data. A test was conducted as follows. The flywheel was driven to 1100 rpm, at which time pump P_1 was shut off and V_1 was turned ON. The pump/motor PM_2 functioned as a hydraulic pump with maximum displacement, but the pressure difference between the inlet and outlet ports was small because fluid was moving in a cycle from the low-pressure accumulator via PM_2 and back to the low-pressure accumulator. A few identical tests were conducted to test the repeatability. The results of the simulation and experiment are shown in Fig. 9, which indicates agreement. Under the test conditions, the energy of the flywheel was significantly reduced for times longer than 10 seconds. However, the braking time in most applications is only a few seconds, so the system can still be considered suitable as a regenerative energy simulator system.

5.2 Energy recovery potential of system

5.2.1 Influence of overall efficiencies of system components

A cycle of energy recovery is defined as follows. The kinetic energy of the flywheel is transferred to the accumulator as potential energy in the form of high-pressure fluid, which then transforms the stored energy back into kinetic energy via the flywheel. Five components participate in the recovery cycle: flywheel – pump – accumulator – motor – flywheel. Round-trip efficiency is defined as the fraction of energy available after reuse and before recovery from the flywheel. This relationship is expressed by Eq. (36),

$$\eta_{rt} = \eta_{fl,d}\eta_p\eta_{ac}\eta_m\eta_{fl,a} \tag{36}$$

where η_{fl} is the efficiency of the flywheel, $\eta_{m/p}$ is the efficiency of the pump/motor, and η_{ac} is the efficiency of the accumulator. The efficiencies of the flywheel during deceleration ($\eta_{fl,d}$) or acceleration ($\eta_{fl,a}$) in Eq. 36 depends on the char-
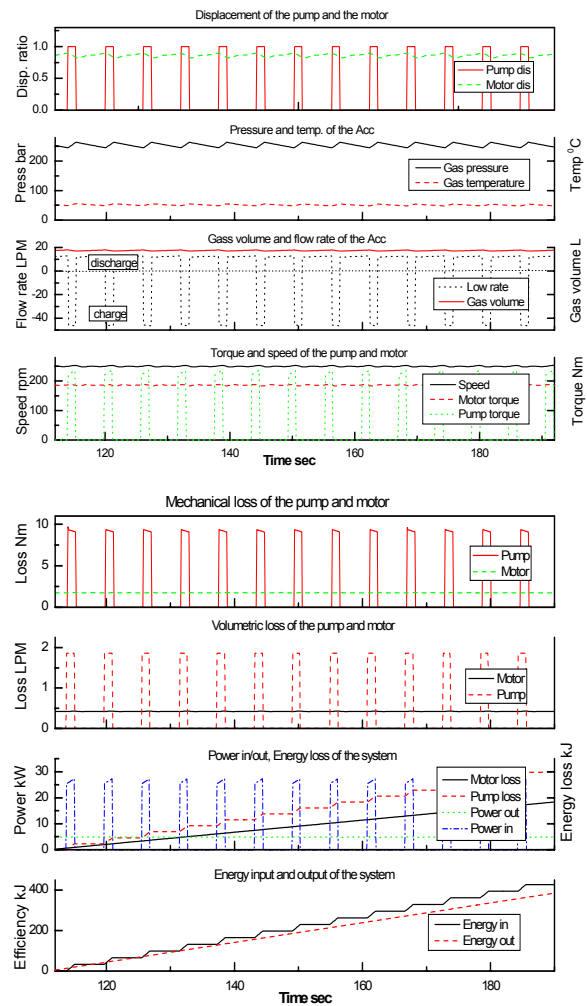

Fig. 8. Parameters of pressure coupling configuration and ON/OFF control strategy.

acteristics of the particular load. The efficiencies of the flywheel as functions of friction forces and the accelerator are assumed to be constant and similar during both deceleration and acceleration. Determination of the efficiency based on Fig. 9 is as follows. Assuming a deceleration time of 3 seconds, the energy of the flywheel decreases from $E_0 = \frac{1}{2}J\omega_0^2$ to $E_3 = \frac{1}{2}J\omega_3^2$ after 3 seconds, so the efficiency η_{fl} is estimated by Eq. (37) as

$$\eta_{fl} = \frac{E_3}{E_0} = 0.9 \tag{37}$$

The efficiency of the accumulator was assumed to be a constant, 0.95. Fig. 10 shows the round-trip efficiency versus the variation in the pump/motor efficiency. The round-trip efficiency of the test bench varied from 32% to 66% when the motor efficiency was in the interval [0.6 0.94] and the pump efficiency was in the interval [0.68 0.92]. Round-trip effi-
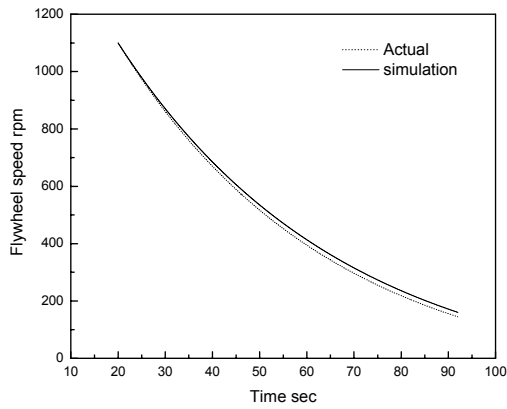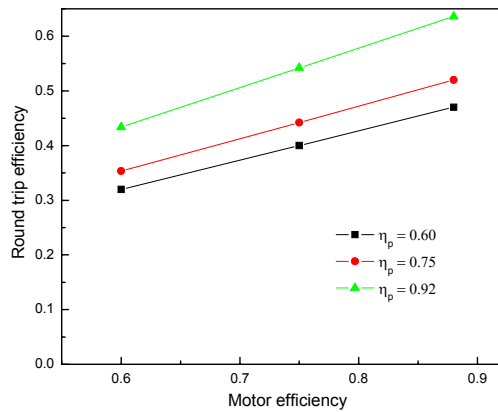
Fig. 9. Flywheel test results.

Fig. 11. (a) Round-trip efficiency versus motor displacement.

Fig. 10. Round-trip efficiency versus pump/motor.
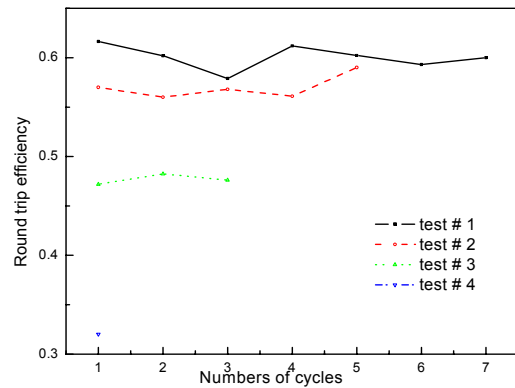
Fig. 11. (b) Round-trip efficiency versus cycling numbers.

ciency requires that the pressure in the accumulator allows the pump/motor to operate in a high-efficiency zone.

The efficiency of the accumulator in practice is not constant and varies according to the charge and discharge cycles. To estimate the influence of the accumulator efficiency on the round-trip efficiency, the pump/motor and flywheel efficiencies were assumed to be constant at 0.85 and 0.9, respectively. The efficiency of the accumulator varied from 0.7 to 0.97. By Equation 36, the round-trip efficiency varied in the range of [0.4 0.56]. To estimate the influence of the load efficiency on the round-trip efficiency, the pump/motor and accumulator efficiencies were again assumed to be constant at 0.85 and 0.9, respectively. The efficiency of the flywheel varied from 0.37 to 0.9 with the changes in the braking time from 20 seconds to 3 seconds, respectively. The round-trip efficiency varied in the range of [0.21 0.52]. In practical applications, the characteristics of the load are known in advance, so the pump/motor and accumulator should be designed for a particular system in order to achieve the highest possible round-trip efficiency.

5.2.2 Influence of pump/motor displacement

For a fixed accumulator with a given pre-charge gas pressure and size, changing the displacement of the pump/motor changes the torque applied to the pump/motor. With small pump/motor displacement, a small torque applied to the
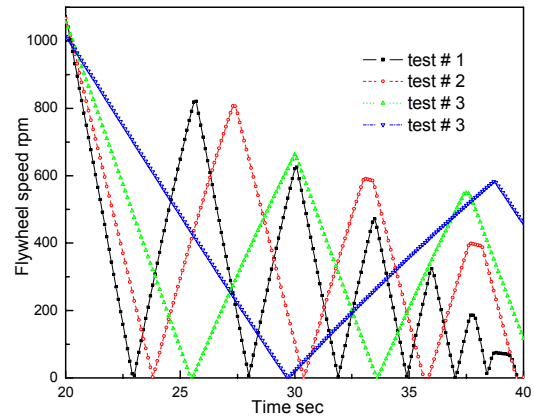
pump/motor results in a large deceleration or acceleration time, and vice versa. Thus, not only the pump/motor efficiency, but also the flywheel and accumulator efficiencies are varied. The energy recovery test procedure was as follows. First, the displacement of the PM_2 was fixed for each test, and the low-pressure accumulator HA_2 was charged to 3 bar by an auxiliary pump (not shown here). The flywheel was driven at 1100 rpm to guarantee that the system achieved a steady-state condition. Next, the pump was shut OFF and valve V_2 was switched to ON instantaneously, while valve V_1 was still OFF. The flywheel ran continuously owing to its kinetic energy. Pump/motor PM_2 functioned as a hydraulic pump. The pressure in the driving line was decreased, and pilot check valve CV_2 was closed. Fluid was pumped from the low-pressure accumulator HA_2 to the high-pressure accumulator HA_1. When the speed of the flywheel reached zero, V_1 was switched to ON. HA_1 became the high-pressure power source, powering PM_2 and functioning as a hydraulic motor. The speed of the flywheel increased while the pressure in HA_1 decreased gradually. During this time, fluid moved from HA_1 to HA_2. When HA_1 was out of energy, the speed of the flywheel was reduced. Then, directional valve V_1 was switched to OFF, but valve V_2 was ON for the next recovery cycle. After some recovery cycles, the reuse maximum speed of the flywheel was reduced due to the characteristics of the fly-

(a) Pump/motor efficiencies

(b) Parameters of high-pressure accumulator

(c) Torque and speed of pump/motor
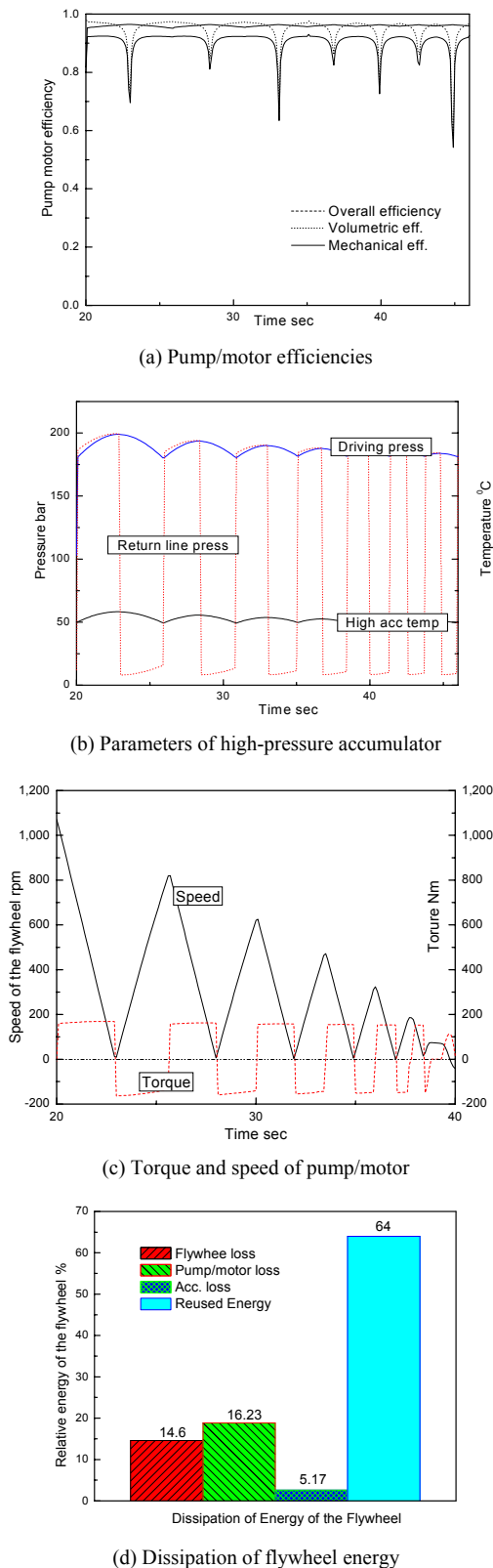

(d) Dissipation of flywheel energy

Fig. 12. Simulation results for system in test number 1.

wheel, and the testing program was stopped. Four motor displacement ratios, 1, 0.75, 0.75, and 0.25, were used in four tests numbered 1, 2, 3, and 4, respectively. To estimate the

energy recovery potential of the system, a parameter called round-trip efficiency was defined as in Eq. (38).

$$\eta_{rt} = \frac{\frac{1}{2} J \omega_{max(i+1)}^2}{\frac{1}{2} J \omega_{max(i)}^2} = \frac{\omega_{max(i+1)}^2}{\omega_{max(i)}^2} \qquad (38)$$

where $\omega_{max(i)}$ i = 0,1… is the maximum speed of the flywheel at recovery cycle i.

The times needed to decelerate the flywheel from maximum speed to zero and to accelerate it from zero to maximum speed are called the braking and accelerating times, respectively. Fig. 11(a) shows the speed curves of the flywheel from our four tests. The braking and accelerating times of the flywheel increased from 2.5 seconds to 10 seconds, respectively, as the displacement ratios decreased from 1 to 0.25. Fig. 11(b) shows the round-trip efficiencies of the system versus the cycle number of the four tests. Test number 4 is not illustrated because only one cycle was conducted, and its value of 0.32 matched that of the previous analysis. The round-trip efficiencies in tests 1 and 2 were quite high, and varied from 55% to 64%.

Fig. 12(a) shows the estimates of the volumetric and mechanical efficiencies of the pump/motor in test 1. In this test, both the mechanical and volumetric efficiencies of the hydraulic pump/motor were high. Fig. 12(b) shows the simulation values for temperature and pressure in the high-pressure accumulator. Fig. 12(c) shows the torque and speed of the pump/motor. Fig. 12(d) shows the dissipation of the kinetic energy in the system, where the initial energy of the flywheel was considered to be 100%. The average efficiency of the pump/motor was about 90%; the energy loss of the flywheel was about 8% for acceleration or deceleration. Fig. 12(d) shows that the loss due to the accumulator was very low (about 5%), that the loss caused by the flywheel was about 14.6%, and that the significant loss due to the pump/motor was nearly 16%, while 64% of the initial energy was reused for flywheel acceleration.

6. Conclusions

A novel energy-saving hydraulic system based on an HST/hydraulic accumulator combination was investigated through analysis and modeling.

A model of the hydraulic pump/motor efficiencies was developed and used to estimate the energy utilization and recovery of the system under different conditions.

The energy utilization of the system was analyzed for three control strategies, indicating that ON/OFF control achieves a high efficiency with a low speed and a high torque ratio, and that the HST mode dominates the others with high values in both speed and torque ratios.

A model validation indicated that the energy recovery potential of the system varied from 32% to 66% depending on the pump/motor displacement. A greater motor displacement

ratio corresponded to a greater energy recovery potential.

In order to confirm the stability of the system, experimental verification by means of a controller for automatic switching between system modes should be undertaken next. .

Acknowledgements

References

[1] D. Manring and G. Luecke, Modeling and Designing a Hydrostatic Transmission With a Fixed Displacement Motor, *ASME,* 120 (1998) 45-49.

[2] A. Njabeleke, R. Pannett, P. Chawdhry and C. Burrows, Self Organising fuzzy logic control of a hydrostatic transmission, *UKACC International Conference on control*, UK. (1998).

[3] Y. Jen and C. Lee, Robust speed control of a pump controlled motor system, *IEE proceeding,* 139 (6) (1992) 503-510.

[4] M. Martelli and L. Zarotti, Hydrostatic Transmission with a Traction Control, *22nd ISARC,* (2005).

[5] H. Schulte, Control Oriented Modeling of Hydrostatic Transmissions using Takagi Sugeno Fuzzy Systems, *Fuzzy Systems Conference, FUZZ-IEEE 2007, IEEE International,* (2007).

[6] K. Dasgupta, Analysis of a hydrostatic transmission system using low speed high torque motor, *Mechanism and machine theory,* 35 (2000) 1481-1499.

[7] R. Kordak, Hydrostatic Drives with Secondary Control, *Bosch Rexroth AG,* (2003).

[8] A. Pourmovahed, N. Beachey and F. Fronczak, Modeling of a Hydraulic Energy Regeneration System – Part I: Analytical Treatment, *ASME,* 114 (1992) 155-159.

[9] A. Pourmovahed, N. Beachey and F. Fronczak, Modeling of a Hydraulic Energy Regeneration System – Part II: Experimental Program, *ASME,* 114 (1992) 160-165.

[10] J. Hao, S. Ikeo, Y. Sakurai and T. Takahashi, Energy Saving of a Hybrid Vehicle Using a Constant Pressure System, *JFPS,* 30 (1) (1999) 20-27.

[11] Y. Yen and C. Lee, Influence of an Accumulator on the Performance of a Hydrostatic Drive with Control of the Secondary Unit, *IMechE.,* 207 (1993) 173-184.

[12] J. Lumkes and F. Fronczak, Design, Simulation, and Validation of a bond graph model and controller to switch Between Pump and Motor Operation Using four ON/OFF Valves with a Hydraulic Axial Piston Pump/Motor, *Proc of the American Control Conference*, USA. (2000) 3605-3609.

[13] H. Yang, W. Sun and B. Xu, New Investigation in Energy Regeneration of Hydraulic Elevators, *IEEE/ASME transaction on mechatronics,* 12 (5) (2007) 519-526.

[14] S. Yokota, T. Nishijima, Y. Kondoh and Y. Kita, A Flywheel Hybrid Vehicle Making Use of Constant Pressure System (Fabrication of Stationary Test Facility and Experiment of Urban Driving Schedule), *JFPS,* 68 (7) (2002) 201-206.

[15] T. H. Ho and K. K. Ahn, A Study on Energy Saving Potential of Hydraulic Control System Using Switching Type Closed Loop Constant Pressure System, *7th JFPS International Symposium on Fluid Power*, Toyama, Japan, (2008) 317-322.

[16] Y. R. Cho and K. K. Ahn, A Study on The Energy Saving Hydraulic System Using Constant Pressure System, *KFPS,* 4 (1) (2007) 7-12.

[17] K. K. Ahn and B. S. Oh, An Experimental Investigation of Energy Saving Hydraulic Control System using Switching Type Closed Loop CPS, *ICFP*, China, (2005) 153-157.

[18] R. Rahmfeld, Development and Control of Energy Saving Hydraulic Servo Drives, *Proceedings of 1st FPNI-PhD Symposium,* Hamburg, (2000) 167-180.

[19] L. Guzzella and A. Sciarretta, Vehicle Propulsion Systems: Introduction to Modeling and Optimization, *Springer*, (2007) .

Triet Hung Ho received B.S. and M.S. degrees from Hochiminh City University of Technology in 2002 and 2004, respectively, both in Mechanical Engineering. He is currently a Doctoral Candidate in the department of Mechanical and Automotive Engineering, University of Ulsan, Ulsan, Korea. His research interests are focused on hydraulic control systems and energy saving in hydraulic systems.

Kyoung Kwan Ahn received a B.S. degree in Mechanical Engineering from Seoul National University in 1990, an M. Sc. degree in Mechanical Engineering from the Korea Advanced Institute of Science and Technology (KAIST) in 1992, and a Ph.D. degree (dissertation title: "A study on the automation of outdoor tasks using 2 link electro-hydraulic manipulator") from the Tokyo Institute of Technology in 1999, respectively. He is currently a Professor in the School of Mechanical and Automotive Engineering, University of Ulsan, Ulsan, Korea. His research interests are design and control of smart actuator using smart material, fluid power control and active damping control. He is a Member of IEEE, ASME, SICE, RSJ, JSME, KSME, KSPE, KSAE, KFPS, and JFPS.